

SiON metrology using angular and energy distributions of photoelectrons

G Tasneem^{1*}, C Tomastik², R Mroczyński³ and W S M Werner⁴

¹Institut für Angewandte Physik, Vienna University of Technology, Wiedner Hauptstrasse 8-10, A-1040 Vienna, Austria

²Austrian Centre for Competence for Tribology, Viktor Kaplan-Straße 2, A-2700 Wiener Neustadt, Austria

³Institute of Microelectronics and Optoelectronics, Warsaw University of Technology, Koszykowa, Poland

⁴Surface and Microanalysis Science Division, National Institute of Standards and Technology, Gaithersburg, MD 20899-8370, USA

*Email: ghazaltasneem@yahoo.com

Abstract. Angle-resolved X-ray photoelectron spectroscopy (ARXPS) is a useful tool for non-destructive in-depth analysis of near surface regions. However, the reconstruction of depth profile from ARXPS data is an ill-posed mathematical problem. Thus, the main goal of this work was to develop a new, iterative algorithm based on the least square fitting which allows to solve this problem. The depth profiles were restored by dividing sample in thin virtual box shaped layers each with a different concentration. To extract information on the depth distribution, this algorithm is based on the analysis of the angular peak intensities along with the inelastic background. In addition, the physically trivial constraint of atomic fractions adding up to unity was imposed. The model takes into account the effect of elastic scattering and anisotropy of the photoelectric cross section. To test the algorithm, experimental spectrum for SiON samples on Si substrate were measured with a Thermo Theta Probe electron spectrometer for off-normal emission angles in the range between 25° and 75°. A very good agreement was found between the measured spectra and obtained spectra from the algorithm.

1. Introduction

Non-destructive methods for obtaining depth profile information from the topmost few nanometres of solids become increasingly important for many technological applications e.g. as the thickness of the nowadays gate dielectric layers used in ULSI CMOS devices, has reached the scale of a fraction of nanometres. Angle-resolved X-ray photoelectron spectroscopy (ARXPS) is widely used for such analysis in order to determine thickness of thin films and the variation of composition of different species with depth [1]. For ARXPS, transformation of the measured photoelectron intensities into a depth profile is not straightforward since inversion of ARXPS data is one of the notorious mathematically ill-posed problems. As much prior knowledge about the sample is utilized to constrain possible solutions and to obtain useful results [1].



In quantitative analysis by ARXPS, the area of the peak of signal electron that have not lost energy while escaping from the target is used for data interpretation after removing the broad background of inelastically scattered electrons. However, recently it was realized (e.g. [2-4]) that not only electrons that haven't lost their energy but the electrons having participated in a given number of inelastic collisions, also contain significant information about the depth distribution of the emitting species. Several methods have been proposed to extract the information about the depth profile from experimental spectra [2-4]. The numerical efforts involved in these methods are generally large and they are mostly based on some kind of least-squares fitting between the entire experimental and theoretical line shapes.

In present paper, a procedure to extract in-depth information from energy and angular distributions of photoelectrons, is introduced.

2. Theory

For a noncrystalline solid, the electron transport in solids may be formulated by a Boltzmann type equation [5-6]. Based on this approach, energy/angular spectrum of emitted electron is given by [5]

$$Y(\mu, E) = T(E) \otimes \sum_{j=0}^n A / \mu \sum_{n=0}^{\infty} \int_0^{\infty} dE' L_n(E - E') f(E') \times \int_0^{\infty} dz P_n(\mu, z) c(z) \quad (1)$$

In this expression, E is the electron energy, μ is the cosine of polar emission angle, θ (with respect to surface normal), $f(E)$ is the true intrinsic spectrum, $c(z)$ is the concentration of the specie at depth z and $T(E)$ represents transmission function of the instrument. The symbol \otimes stand for the convolution operation. Factor A describes the generation rate of signal electrons. The quantity L_n is the partial loss distributions

$$L_n(T) = \int L_{n-1}(T - T') w_b(T') dT' \quad (2)$$

Where $w(T)$ is the distribution of energy loss in a single scattering, E is the electron kinetic energy, and T is the energy loss. The second integral on the right hand side of equation (1) is partial intensity. Partial intensities are the number of electrons that have participated in n inelastic collisions and is denoted by the symbol $C_n(\mu)$. Partial intensity can be defined as

$$C_{ni}(\mu) = \int_0^{\infty} dz P_n(\mu, z) c_i(z) \quad (3)$$

The quantity $P_n(\mu, z)$ represent the partial escape distribution (PED) which account for the inelastic background on the low kinetic energy side of the photo electron peak. PED is defined as [6- 7]: “ The probability distribution for the process in which an electron generated in a certain depth interval will escape from the surface with a direction in a certain angular interval after experiencing a certain number of inelastic scattering processes in solids.” It can be seen from equations 1-3 that partial intensities contain all the information regarding depth profile. Consequently, depth profile can be parameterized by variables $X=(x_1, x_2, \dots, x_i)$. The core of this analysis is determination of these quantities. It should be noted, that depth profile determination is usually greatly facilitated by measuring the yield at several emission angles. Taking above into account, following method acquired data at two different emission angles. Depth profile can be obtained by least square fitting of theoretical spectra to measured raw data by the following function

$$\sum_{i=1}^{n_i} A_i \left[\sum_{j=1}^2 (Y_i^{Sim}(E, \theta_j) - Y_i^{Exp}(E, \theta_j))^2 \right] = 0 \quad (4)$$

Where A is the instrumental factor, i is the specie in the sample, j is angle, Y^{Exp} is the measured spectrum and Y^{Sim} is the simulated spectrum calculated by using equation (1) at two different angles θ_1

and θ_2 respectively. Equation (4) is the system of linear equations and the basis of proposed methods for retrieval of depth profile.

3. Experimental

Two-inch $\langle 100 \rangle$ *p* type silicon substrates of the resistivity 4-7 Ωcm were used in this study. The silicon oxynitride films were fabricated in an Oxford Plasma Technology PLASMALAB 80+ system. The silicon substrates before the experiments were cleaned using the standard RCA method. The parameters of plasma enhanced chemical vapor deposition (PECVD) process were optimized to allow repeatable formation of dielectric films. The PECVD process runs in parallel plate reactor in a RF-plasma (13.56 MHz). Process parameters necessary for ultra-thin oxynitride to be formed are presented in table 1. In this paper the following names are used to refer to the types of ultra-thin dielectric layers studied: 'SiO_x' and 'SiO_xN_y' for sample with very low and significantly higher content of silicon nitride phase, respectively (see table 1).

Table 1. Process Parameters allowing formation of ultra-thin PECVD dielectric layers

	SiO _x	SiO _x N _y
Power [W]	10	10
Pressure [m Torr]	350	400
SiH ₄ flow [sccm] (diluted 2% in N ₂)	100	150
N ₂ O flow [sccm]	150	16
NH ₃ flow [sccm]	-	32

The ARXPS measurements were collected using a Theta Probe instrument, a method of parallel ARXPS measurements. Monochromated Al K α X-ray source ($h\nu \approx 1486.6$ eV) was used throughout the work. The samples were introduced into the ultrahigh vacuum chamber that had a base pressure of $\approx 10^{-10}$ mbar and measurement pressure of $\approx 10^{-9}$ mbar ($\approx 10^{-7}$ Pa) after cleaning by sputtering with 1 keV Ar⁺ ions. The angular distributions were measured for emission angle (perpendicular to the surface normal) of 25° to 75° with a step size of 10°.

In the present study, surface losses were removed from each measured spectrum. The spectrum deconvolution procedure of Werner [7-9] was applied repeatedly to a spectrum until the background due to surface losses was eliminated in the considered energy range:

$$Y_{k+1} = Y_k(E) - q_{k+1} \int Y_k(E+T)L_{k+1}(T)dT \quad (5)$$

Where Y_k is the spectrum from which *k*-fold scattering has been eliminated. The coefficients q_k are functions of the reduced partial intensities, $c_n = C_n/C_0$, where the partial intensities C_n represent the number of electrons that reach the detector after *n*-fold inelastic scattering and C_0 represents the number of electrons that reach the detector without inelastic scattering:

$$\begin{aligned}
 q_1 &= c_1 \\
 q_2 &= c_2 - q_1^2 \\
 q_3 &= c_3 - q_1 q_2 - q_1^3 \\
 q_4 &= c_4 - q_1 q_3 - q_2^2 - q_1^2 q_2 - q_1^4
 \end{aligned}
 \tag{6}$$

The kernels used in equation (5) for each stage of the deconvolution are shown in figure 1 and figure 2 for O1s and Si (2p, 2s) peaks. The differential surface excitation probability (DSEP) provide the function $w_s(T)$ (for deconvolution of surface-inelastic scattering) and were taken from reference. [10].

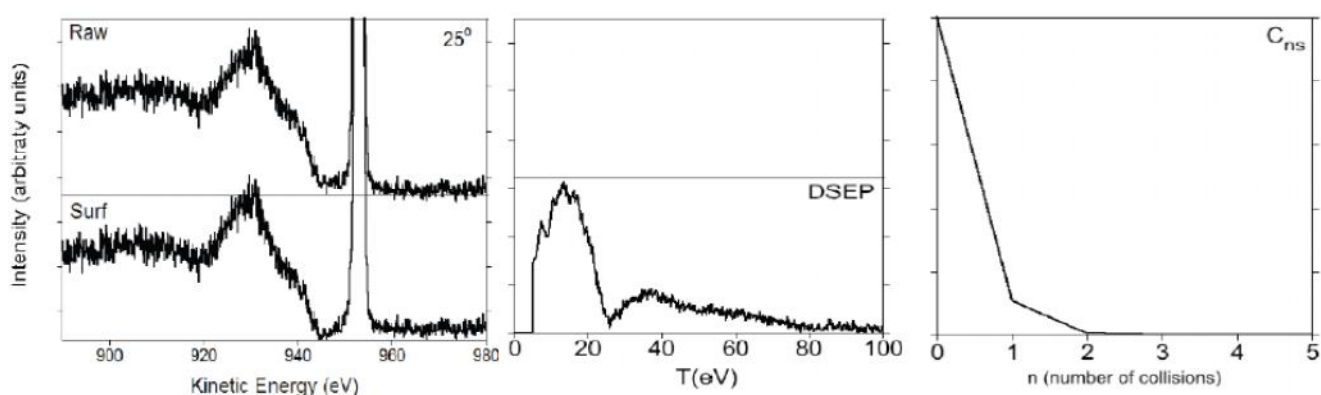


Figure 1. Kernel used for O1 s

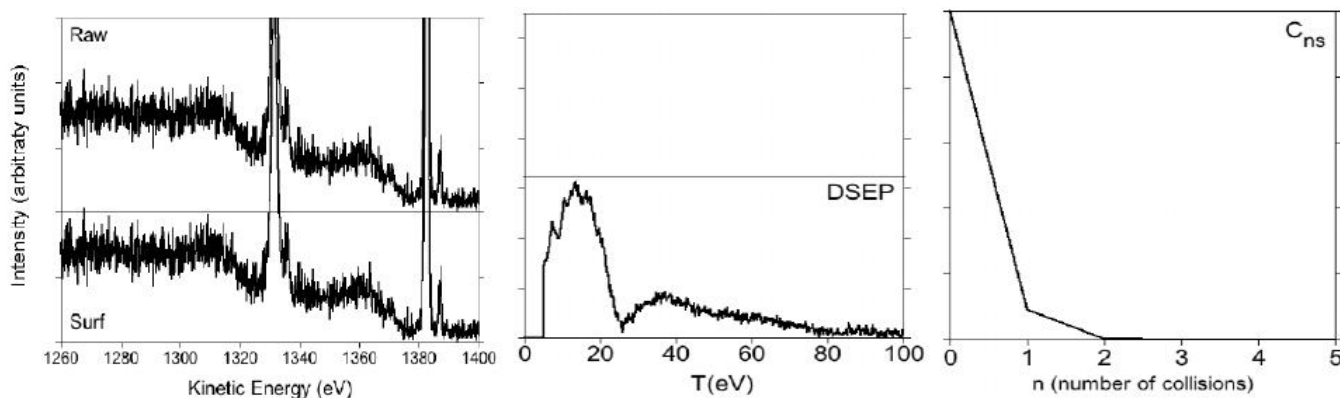


Figure 2. Kernel used for Si 2p

4. Results and Discussion

To analyze the performance of the proposed method described above, experimental data were used for SiOx and SiOxNy films on the Si substrate with C contamination at the top. Present model includes the effect of anisotropy in the photoionization cross-section and elastic scattering. The spectrums were calculated by using least square fitting at the emission angles of 25° and 55°. The partial intensities were

calculated by using Simulation of Electron Spectra for Surface Analysis (SESSA) [11,12]. The obtained thickness of the films and concentrations of particular component in each layer is in table 2 and 3 for SiO_x and SiO_xN_y respectively. Figure 3 and 5 shows the comparison of the calculated (dashed lines) and experimental spectrum (solid lines) after removal of surface excitations. There is a good agreement between experimental and calculated spectrum for all analyzed samples and the emission angles of 25° and 55°. Figure 4 and 6 shows the comparison of the experimental and calculated peak intensities after normalization. Experimental and calculated peak intensities generally agree well for all emission angles except the angles greater than 70°.

Table 2. Obtained thickness and concentration of particular component in each layer for SiO_x

Sample 1	Thickness (nm)	Chemical Specie
Layer 1	0.1	C
Layer 2	8.0	Si _{0.4} O _{0.6}
Layer 3	Substrate	Si

Table 3. Obtained thickness and concentration of particular component in each layer for SiO_xN_y

Sample 1	Thickness (nm)	Chemical Specie
Layer 1	0.15	C
Layer 2	1.0	Si _{0.455} O _{0.545}
Layer 2	3.5	Si _{0.44} O _{0.34} N _{0.22}
Layer 3	Substrate	Si

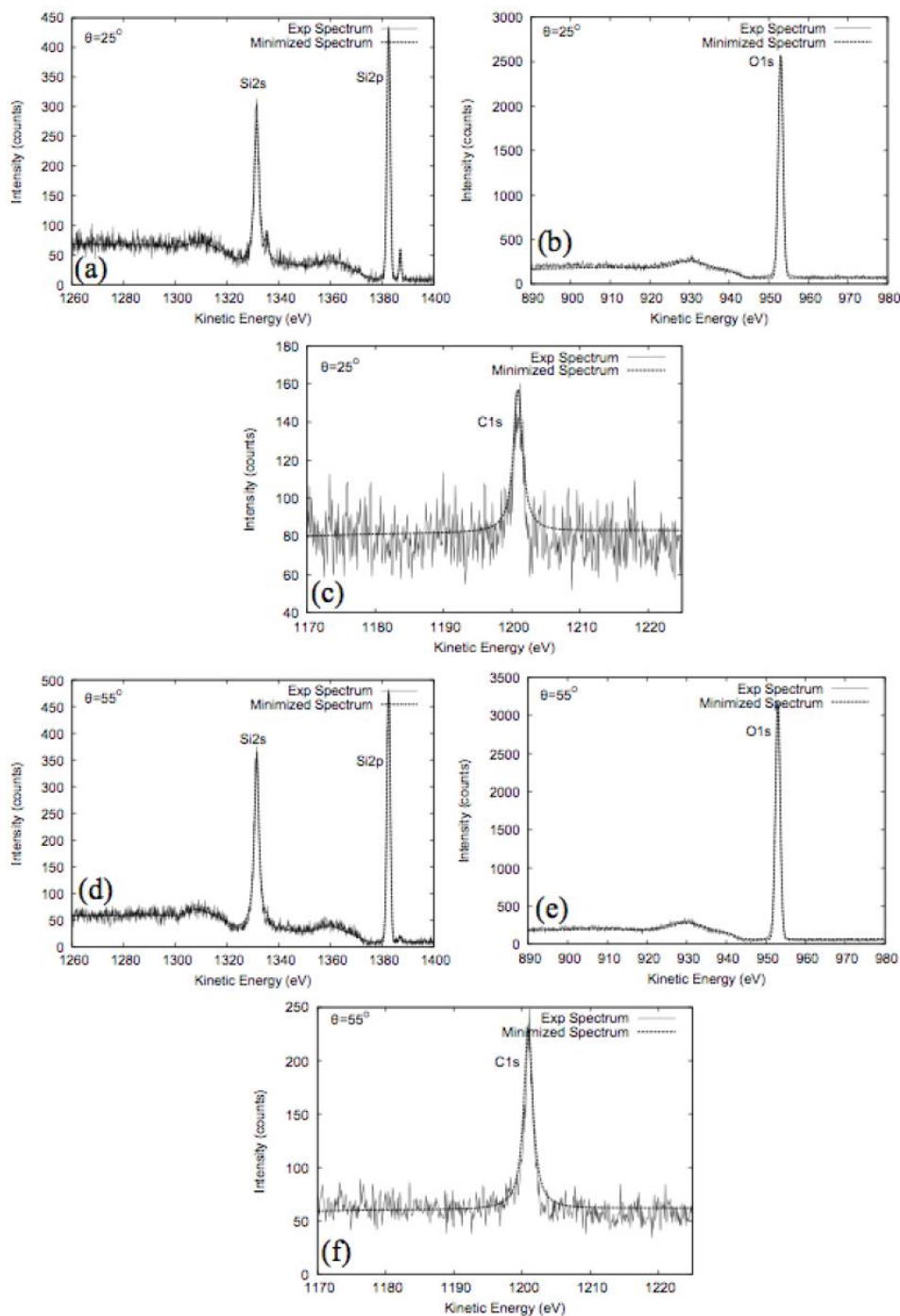


Figure 3. Fitting of Experimental spectrum and simulated spectrum at emission angle of 25° and 55° for Sample 1. (a) Si 2p and Si 2s spectrum at 25° . (b) O 1s spectrum at 25° . (c) C 1s spectrum at 25° . (d) Si 2p and Si 2s spectrum at 55° . (e) O 1s spectrum at 55° . (f) C 1s spectrum at 55°

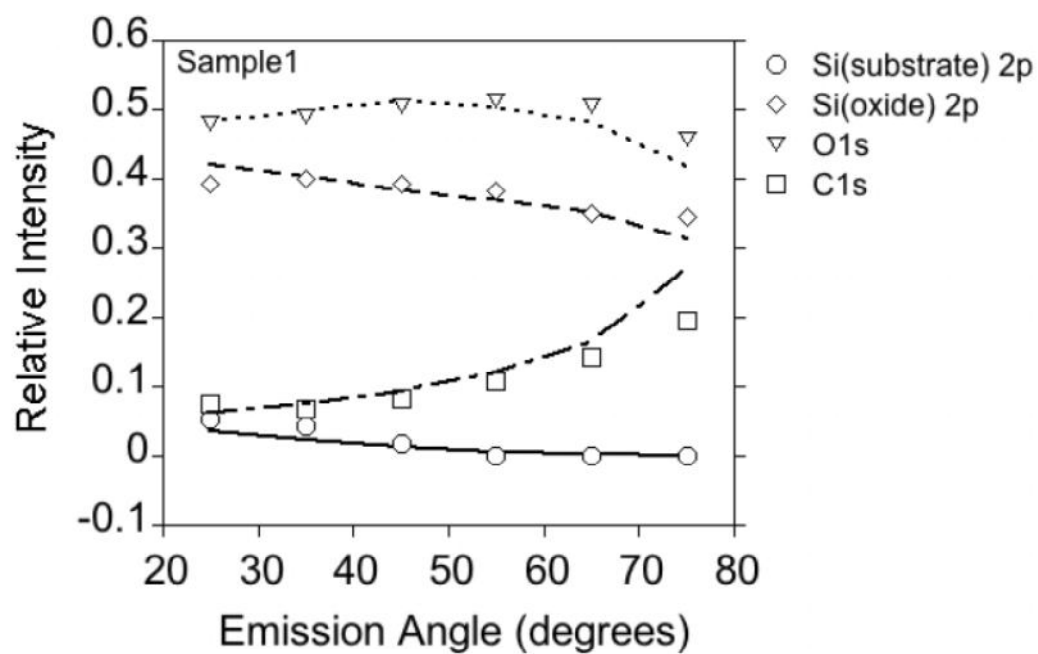


Figure 4. Comparison of experimental and calculated AR normalized peak intensities

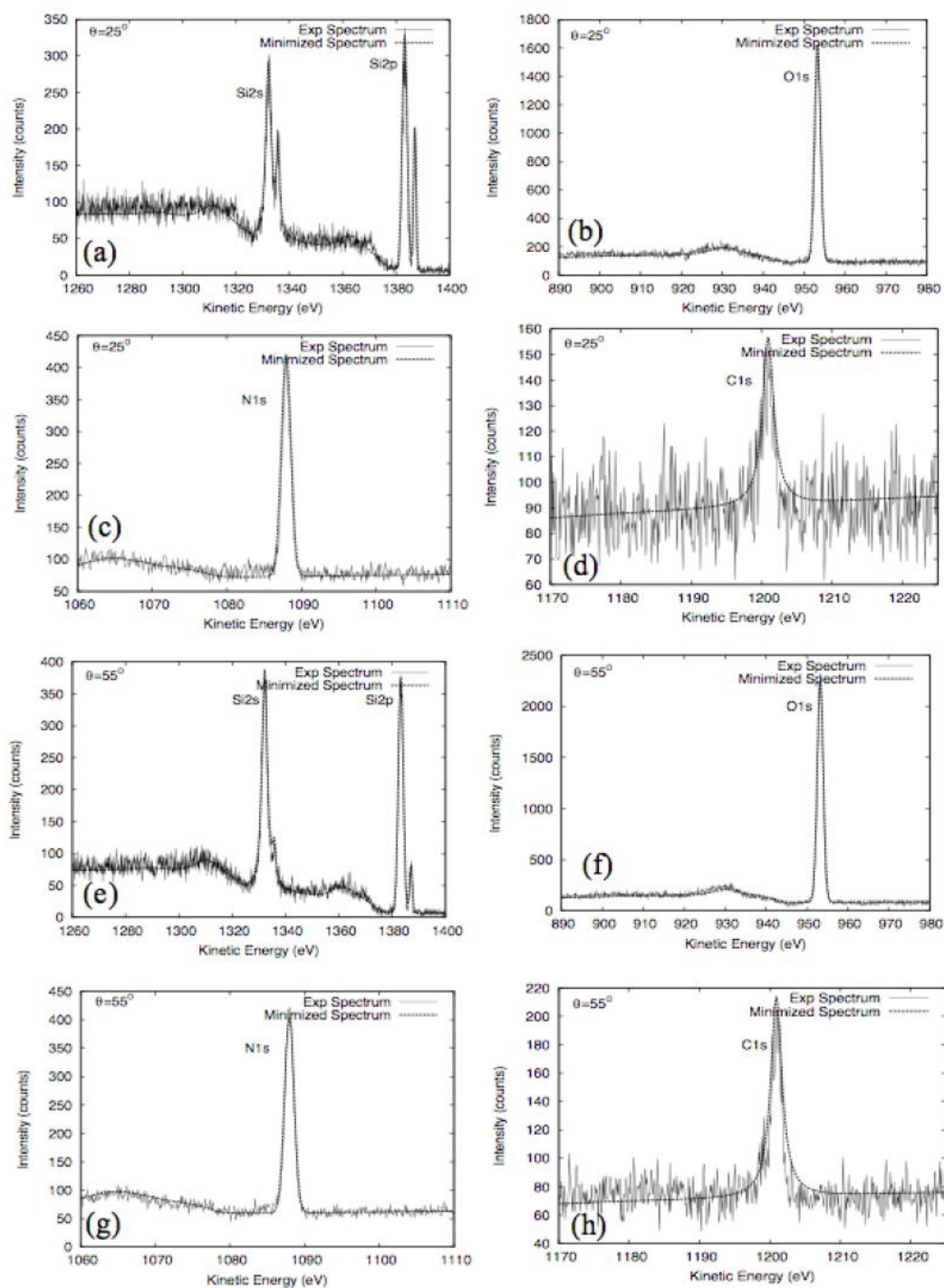


Figure 5. Fitting of Experimental spectrum and simulated spectrum at emission angle of 25° and 55° for Sample 2. (a) Si 2p and Si 2s spectrum at 25° . (b) O1s spectrum at 25° . (c) N1s spectrum at 25° . (d) C1s spectrum at 25° . (e) Si 2p and Si 2s spectrum at 55° . (f) O1s spectrum at 55° . (g) N1s spectrum at 55° . (h) C1s spectrum at 55°

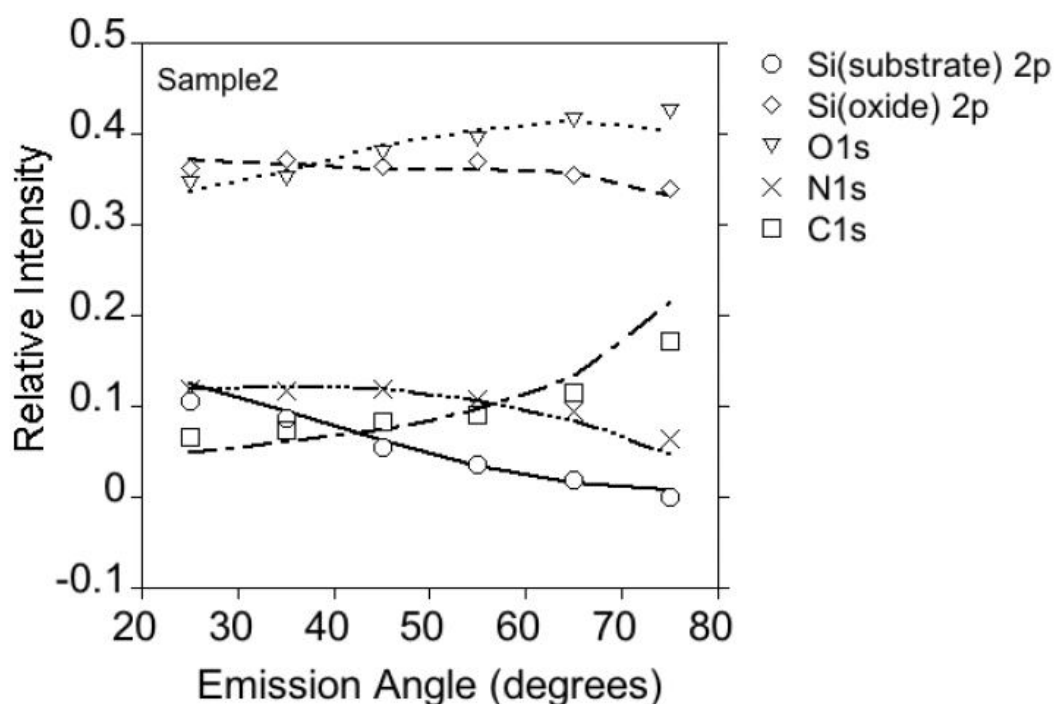


Figure 6. Comparison of experimental and calculated AR normalized peak intensities

5. Conclusions

Compositional depth profile can be retrieved accurately by using energy and angular distributions. Angular distribution in the Theta Probe configuration can only be quantitatively interpreted with a model that accounts for elastic scattering of the photoelectron as well as anisotropy of the photoionization cross section.

References

- [1] Cumpson P J 2003 In Surface Analysis by Auger and X-ray Photoelectron Spectroscopy (Eds: Briggs D and Grant J T) *IM Publications, Chichester* 651
- [2] Tougaard S 1986 *Surf. Interface Anal.* **8** 257
- [3] Tougaard S and Hansen S H S 1989 *Surf. Interface Anal.* **14** 730
- [4] Werner WSM 1995 *Surf. Interface Anal.* **B 23** 696
- [5] Werner WSM, Tilinin I S, Beilschmid H and Hayek M 1994 *Surf. Interface Anal.* **B 21** 537
- [6] Tilinin S and Werner WSM 1993 *Surf. Sci.* **290** 119
- [7] Werner WSM, 1995 *Phys. Rev.* **B 52** 2964
- [8] Werner WSM, 1995 *Surf. Interface Anal.* **23** 737
- [9] Werner WSM 2001 *Surf. Interface Anal.* **31** 141
- [10] Werner WSM, Glantschnig K and Ambrosch-Draxl C 2009 *J. Phys. Chem. Ref. Data* **38** 1013
- [11] <http://www.nist.gov/srd/nist100.htm>.
- [12] Smekal W, Werner WSM and Powell CJ 2005 *Surf. Interface Anal.* **37** 1059